PNAS
www.pnas.org

Supplementary Information for
The K63 deubiquitinase CYLD modulates autism-like behaviors and hippocampal plasticity by regulating autophagy and mTOR signaling

Elisa Colombo, Guilherme Horta, Mona K. Roesler, Natascha Ihbe, Stuti Chhabra, Konstantin Radyushkin, Giovanni Di Liberto, Mario Kreutzfeldt, Sven Schumann, Jakob von Engelhardt, Doron Merkler, Christian Behl, Thomas Mittmann, Albrecht M. Clement, Ari Waisman and Michael J. Schmeisser

Ari Waisman, Michael J. Schmeisser
Email: waisman@uni-mainz.de; mschmeisser@uni-mainz.de

This PDF file includes:

Figures S1 to S7

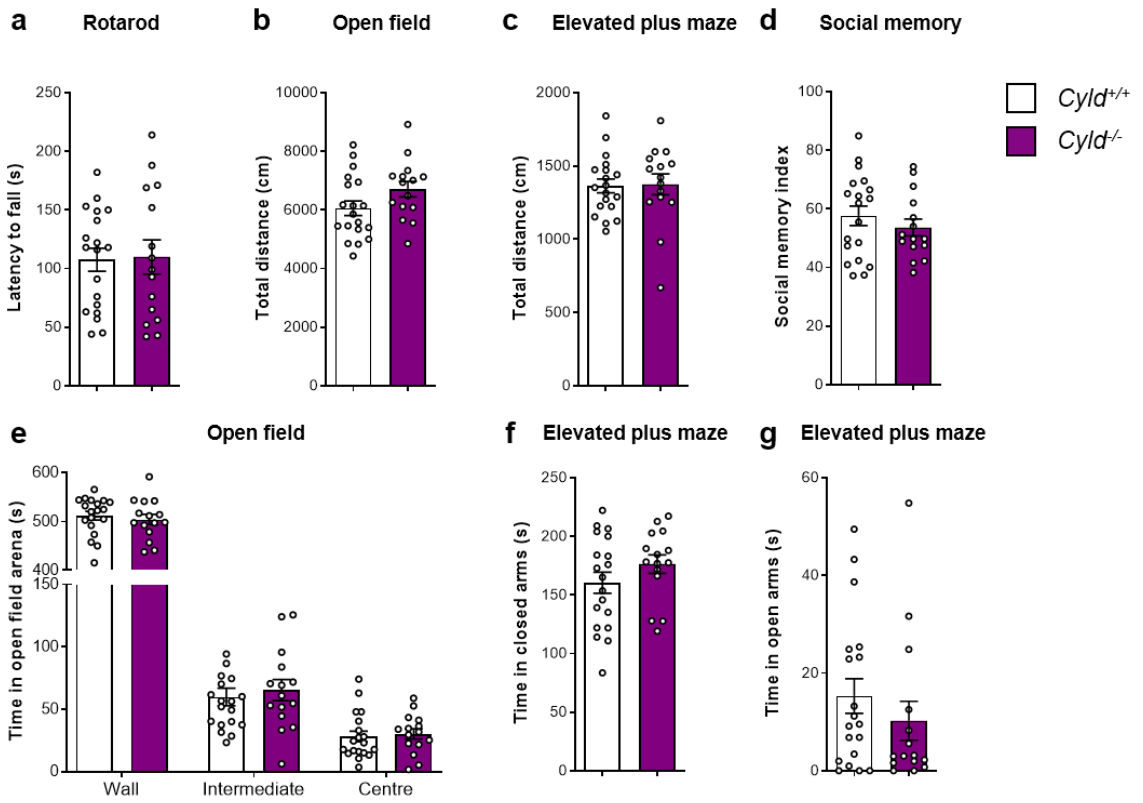

Fig. S1. Behavioral analysis of motor function, anxiety and social memory in *Cyld*$^{-/-}$ mice. **a** Latency to fall from rotating rod, measured in the rotarod test. **b-c** Total distance travelled in Open field and Elevated plus maze tests. **d** Social index parameter analyzed for social memory in the three-chamber test. **e** Open field analysis with time in arena areas. **f-g** Elevated plus maze analysis with time in closed and open arms. For experiments in a-g, n = 19 for *Cyld*$^{+/+}$ controls and n = 15 for *Cyld*$^{-/-}$ mice. All n values used for statistics refer to the number of mice used, after identification of possible outliers with Grubbs' method. For experiments a-g statistics calculated by unpaired nonparametric Mann-Whitney test. Graphs are mean ± s.e.m.

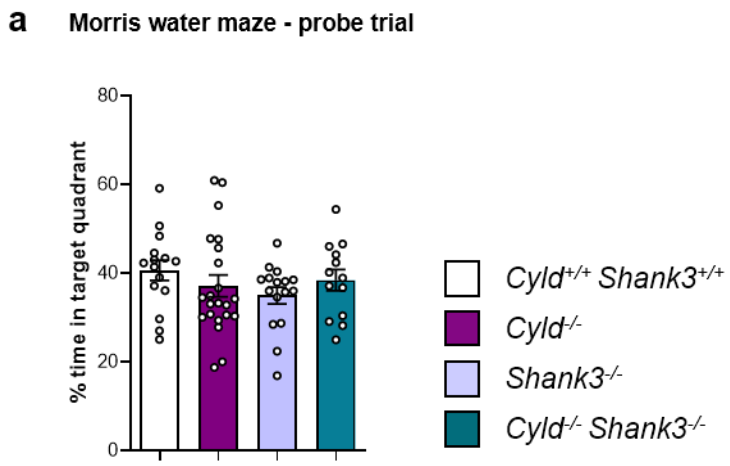

Fig. S2. Morris Water Maze probe trial analysis of *Cyld*$^{-/-}$, *Shank3*$^{-/-}$, and *Cyld*$^{-/-}$*Shank3*$^{-/-}$ double mutant mice (**a**). For experiments in a, n = 15 for *Cyld*$^{+/+}$*Shank3*$^{+/+}$ controls, n = 22 for *Cyld*$^{-/-}$ mice, n = 17 for *Shank3*$^{-/-}$, and n = 13 for *Cyld*$^{-/-}$*Shank3*$^{-/-}$ mice, from 4 independent cohorts. The percentage of time spent in the target quadrant during the probe trial showed no differences. Graph is mean ± s.e.m.

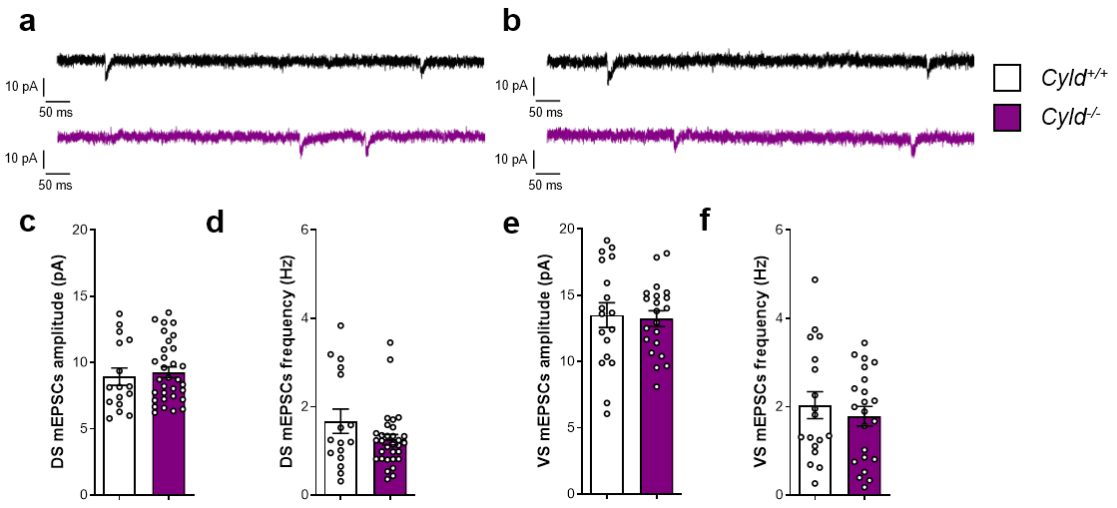

Fig. S3. mEPSC currents in striatal medium spiny neurons (MSNs) are not changed upon loss of CYLD. **a-b** Representative voltage traces of pharmacologically isolated AMPA receptor-mediated mEPSCs in dorsal striatum (DS, **a**) and ventral striatum (VS, **b**), respectively. **c-f** Quantification of mEPSC frequency and amplitude in DS and VS of *Cyld*$^{-/-}$ mice and *Cyld*$^{+/+}$ controls at P42. For experiments in c-d, n = 16 neurons from *Cyld*$^{+/+}$ controls and n = 32 neurons from *Cyld*$^{-/-}$ mice. For experiments in e-f, n = 18 neurons from *Cyld*$^{+/+}$ controls and n = 22 neurons from *Cyld*$^{-/-}$ mice. Statistics calculated by unpaired t-test show no significant differences. Graphs are mean ± s.e.m.

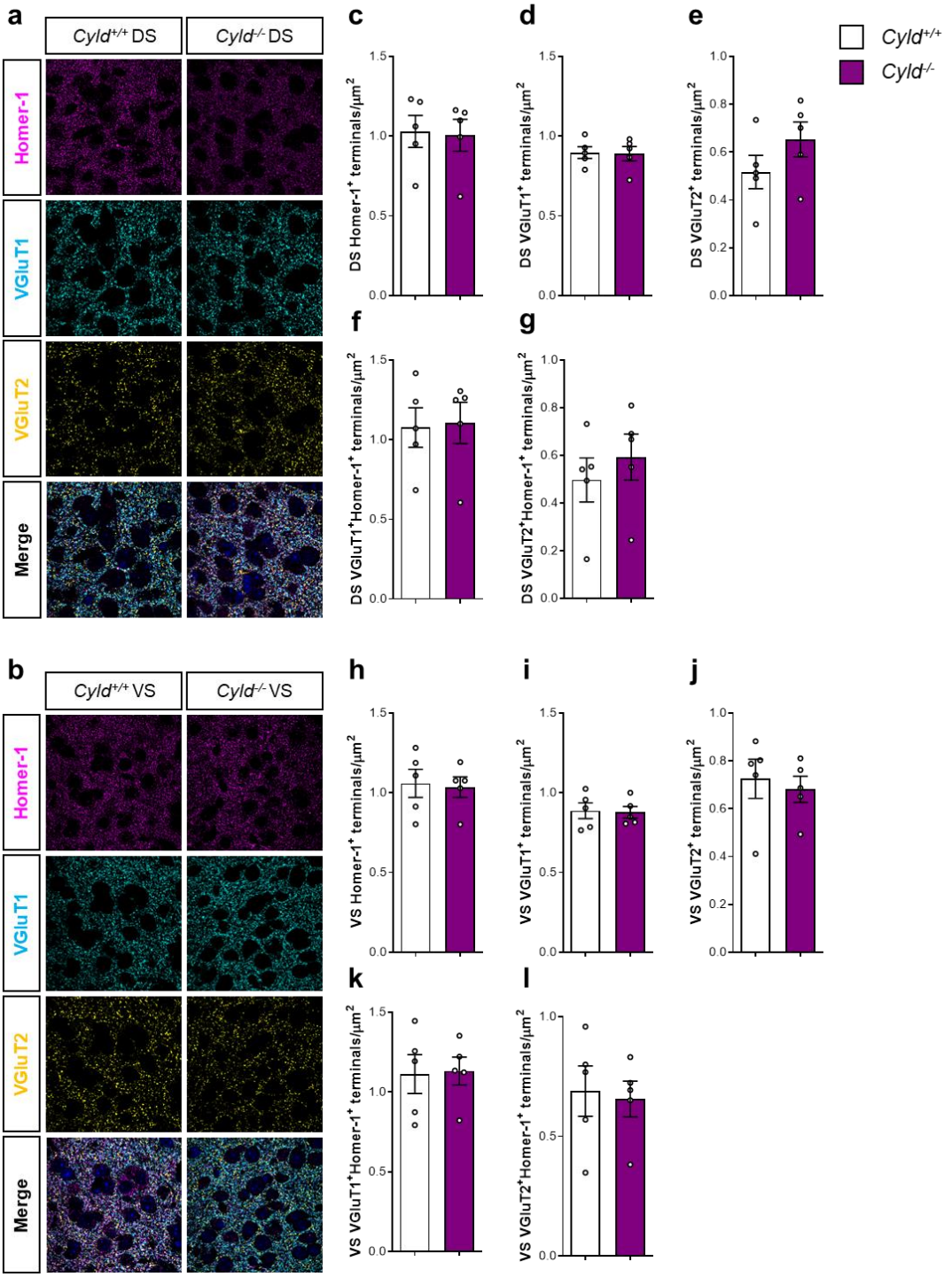

Fig. S4. The densities of cortico- and thalamostriatal excitatory inputs to the dorsal (DS) and ventral (VS) striatum are not altered in *Cyld*$^{-/-}$ mice. **a-b** Representative staining for excitatory synaptic terminals with pre-synaptic VGluT1 (corticostriatal) and VGluT2 (thalamostriatal), and post-synaptic Homer-1. **c-l** Quantification of both single synaptic marker and colocalization analysis of pre- and post-synaptic markers in DS and VS of *Cyld*$^{-/-}$ and *Cyld*$^{+/+}$ control mice. For experiments in a-l, n = 5 for *Cyld*$^{+/+}$ controls and n = 5 for *Cyld*$^{-/-}$ mice at P42. Statistics calculated by unpaired t test, show no significant differences. Graphs are mean ± s.e.m.

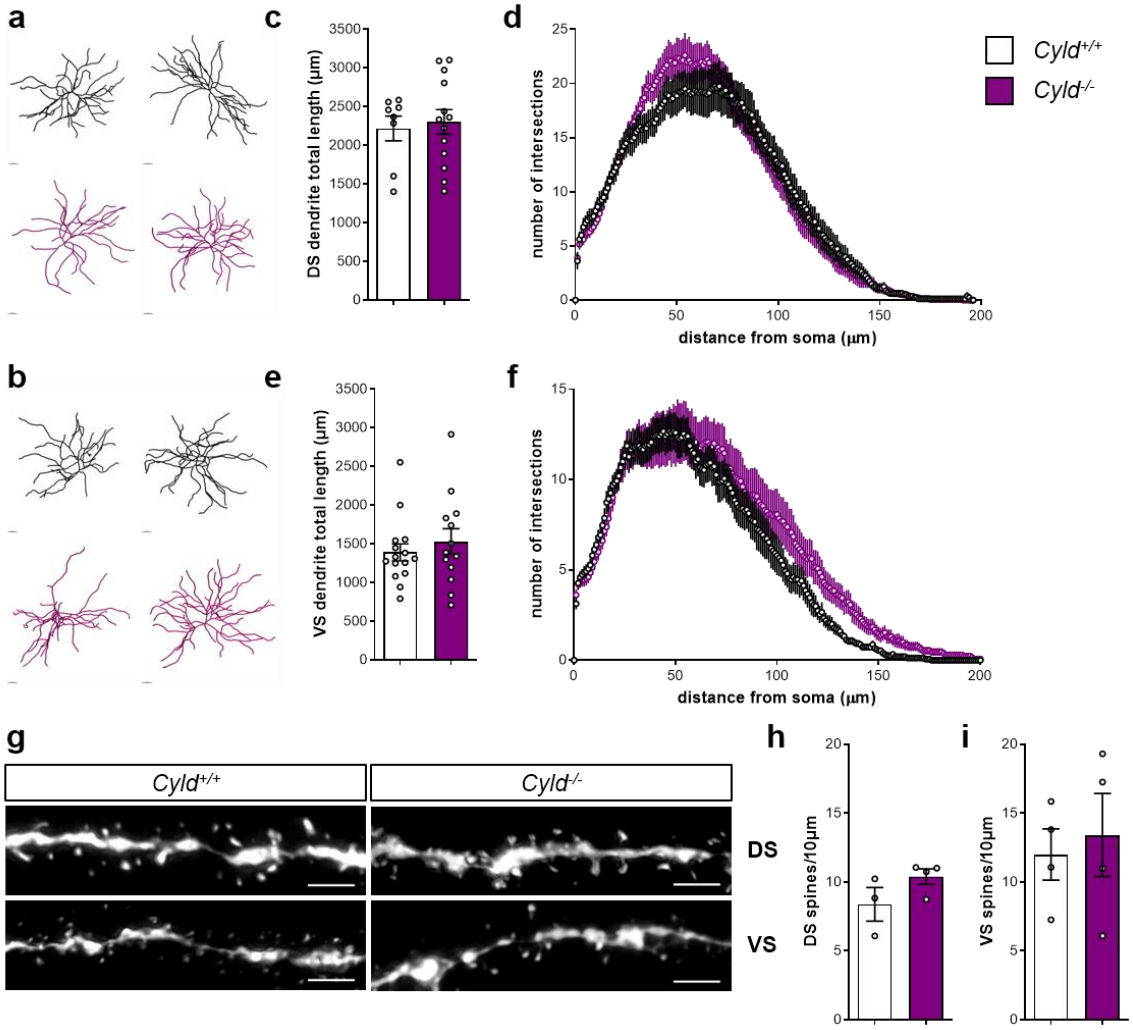

Fig. S5. MSN morphology in dorsal and ventral striatum do not differ between *Cyld*$^{-/-}$ mice and controls. **a-b** Representative pictures of reconstructed biocytin filled MSNs by IMARIS at P42 in DS and VS, respectively. **c-f** Measure of dendrite total length and Sholl analysis of reconstructed MSNs in DS and VS. **g-i** Representative pictures of MSN dendrites and quantification of spine number in DS and VS of *Cyld*$^{-/-}$ mice and *Cyld*$^{+/+}$ controls. For experiments in c-d, n = 8 neurons from *Cyld*$^{+/+}$ controls and n = 13 neurons from *Cyld*$^{-/-}$ mice. For experiments in e-f, n = 15 neurons from *Cyld*$^{+/+}$ controls and n = 13 neurons from *Cyld*$^{-/-}$ mice. For experiments in h-i, n = 4 for *Cyld*$^{+/+}$ controls and n = 4 for *Cyld*$^{-/-}$ mice. Statistics calculated by unpaired t test (c, e, h-i), and two-way repeated-measures analysis of variance (ANOVA) with Sidak's (d, f) post-hoc tests show no significant differences. Graphs are mean ± s.e.m. Error bars in a-b = 20 µm, error bars in g = 5 µm.

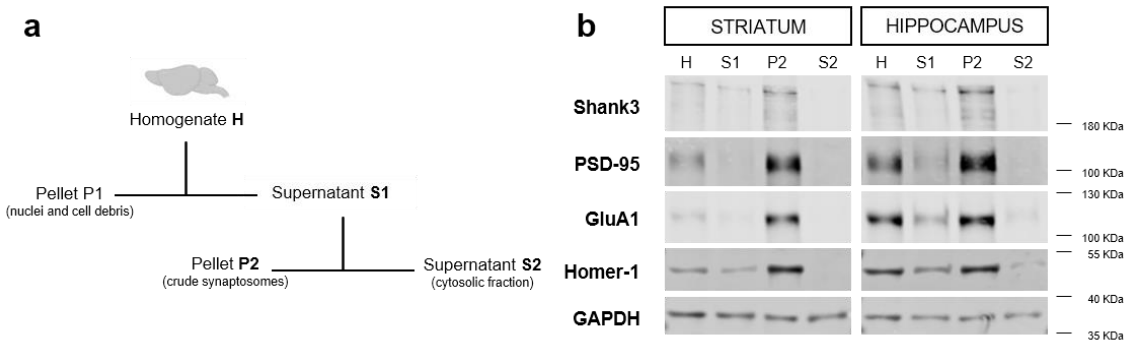

Fig. S6. Crude synaptosome fraction (P2) isolation from mouse striatum and hippocampus. **a** Schematic representation of the workflow for the isolation of crude synaptosome fraction, described in the material and methods section. **b** SDS-PAGE of the isolation steps till crude synaptosome fraction blotted on a 7.5% gel, showing the enrichment of specific synaptic proteins, such as Shank3, PSD-95, GluA1 and Homer-1.

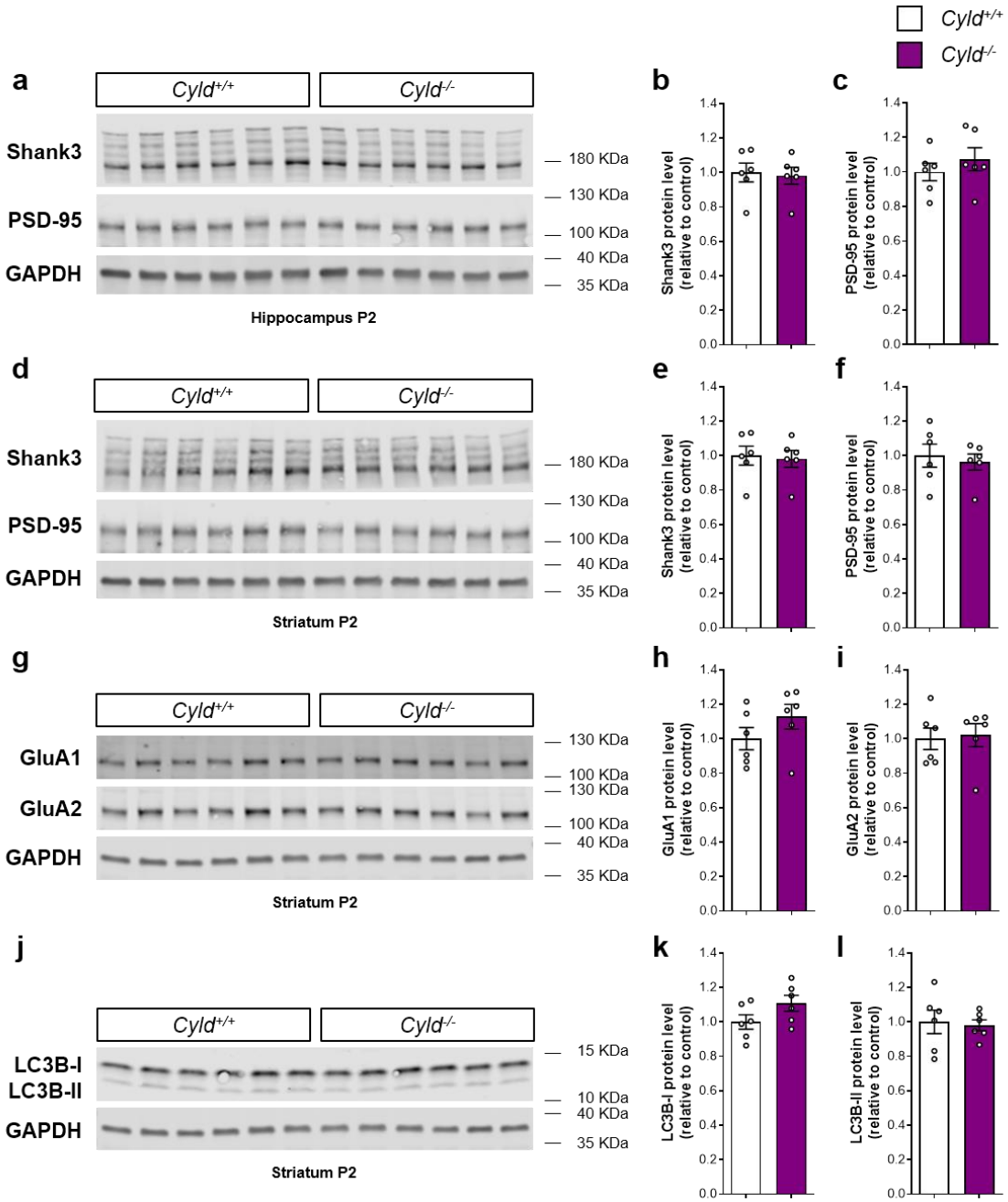

Fig. S7. Biochemical analysis of specific postsynaptic proteins in the striatal and hippocampal P2 fraction with no changes in *Cyld*$^{-/-}$ mice. **a-f** Western blot analysis of Shank3 and PSD-95 normalized to GAPDH in the hippocampal and striatal P2 fraction. **g-i** Western blot analysis of AMPA receptor subunits GluA1 and GluA2 each normalized to GAPDH in the striatal P2 fraction. **j-l** Western blot analysis of LC3B-I and LC3B-II each normalized to GAPDH in the striatal P2 fraction. Lysates (20 µg proteins) of *Cyld*$^{-/-}$ mice and *Cyld*$^{+/+}$ controls were run on a 4-15% gradient gel. GAPDH control is the same for g and j; GluA1, GluA2, and LC3B signals are coming from the same membrane. For experiments in a-l, n = 6 for *Cyld*$^{+/+}$ controls and n = 6 for *Cyld*$^{-/-}$ mice at P42. Statistics calculated by unpaired t test, show no significant differences. Graphs are mean ± s.e.m.